Journal of Applied Sciences

ISSN 1812-5654

science alert

ANSInet
an open access publisher
http://ansinet.com

Journal of Applied Sciences 8 (13): 2369-2377, 2008
ISSN 1812-5654

Modeling, Dynamic Analysis and Optimization of Budsan Truck Engine Mount

Seyed Ahmad Mireei, Seyed Saeid Mohtasebi, Mahmoud Omid and Reza Alimardani
Department of Agricultural Machinery Engineering, University of Tehran, Karaj, Iran

Abstract: This research presents dynamic and vibrating analysis of Budsan truck engine mount. First the system equations are presented and solved by MATLAB. After that, the dynamic forces exerted on the system are obtained and used for the harmonic analysis. Then the FEM results are compared with analytical model results to verify analytical model. Finally, the optimum stiffness as well as the damping of the system are presented and discussed to reduce the system vibration and avoid the resonance phenomena. The results show that an increase in the stiffness of the system from 2943 to 5500 kN would reduce the displacement from 7 to 3.5 mm and an increase of the stiffness to 5500 kN and a hystersis from 0.285 to 0.5 could reduce the displacement from 7 to 2 mm.

Key words: Budsan truck, engine mount, vibration analysis, dynamic analysis, natural frequencies

INTRODUCTION

The major functions of the engine mounting system are to support the weight of the engine and to isolate the unbalanced engine disturbance force from the vehicle structure. For an internal combustion engine, there exist two basic dynamic disturbances: (a) the firing pulse due to the explosion of the fuel in the cylinder and (b) the inertia force and torque caused by the rotating and reciprocating parts (piston, connecting rod and crank). The firing pulses will cause a torque to act on the engine block about an axis parallel to the crank. The directions of the inertia forces are both parallel to the piston axis and perpendicular to the crank and piston axes. For a multi-cylinder engine, the components of the engine-unbalanced disturbance depend on the number and arrangement of the cylinders in the engine. These engine disturbances will excite the engine six Degree of Freedom (DOF) vibration modes as shown in Fig. 1 (Yu *et al*., 2000).

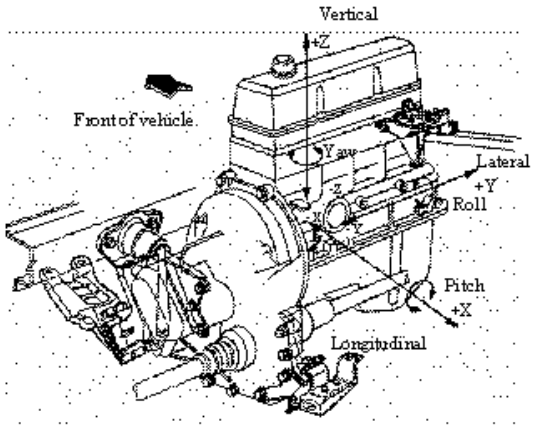

Fig. 1: Engine six DOF modes

In order to obtain a low transmissibility, the natural frequency of the mounting system in a certain direction must be below the engine disturbance frequency of the engine idle speed to avoid excitation of mounting system resonance during normal driving conditions. This means that the engine mount stiffness coefficient should be as low as possible to obtain a low transmissibility. If the elastic stiffness of the engine mount is too low, then the transient response (of the engine mount system) can be problematic for the shock excitation. Shock excitation would be a result of sudden acceleration and deceleration, braking and riding on uneven roads. So from this point of view, high stiffness and high damping are required to minimize the engine motion and absorb engine shake and resonance.

From the above discussion, it can be easily inferred that to isolate the engine vibration in a relatively high frequency range, the engine mounts are required to be soft-low elastic stiffness and low damping and to prevent engine bounce in the low frequency range, engine mounts should be hard-high elastic stiffness and high damping (Yu *et al*., 2000).

Elastomeric (or rubber) mounts have been widely used to isolate vehicle structure from engine vibration since the 1930s (Browne and Taylor, 1939). Since then,

Corresponding Author: Seyed Saeid Mohtasebi, Department of Agricultural Machinery Engineering, Faculty of Biosystems Engineering, University of Tehran, P.O. Box 4111, Postal Code 31587-11167, Karaj, Iran Tel: 0098912-1066902 Fax: 0098261-2801011

much significant advancement, were made to improve the performance of the elastomeric mounts (Browne and Taylor, 1939; Bucksbee, 1987). Elastomeric mounts can be designed for the necessary elastic stiffness rate characteristics in all directions for proper vibration isolation. They are compact, cost-effective and maintenance free. The elastomeric mount can be modeled by Voigt model which consists of a spring and a viscous damper (Swanson, 1992).

The objective of the engine mount optimization should be clear in advance of realizing any optimization procedure. Different objectives of optimization have been considered in the literatures. One objective of optimization is to tune the natural frequency of the engine mounting system to some desired range to avoid resonance and to improve the isolation of vibration and noise and shock excitations (Arai *et al*., 1993; Johnson and Subhedar, 1979). Johnson and Subhedar (1979) proposed a design objective, which tunes all of the system natural frequencies to 6-16 Hz and decouples each mode of vibration through dynamic analysis and optimization. Geck and Patton (1984) proposed a lower roll natural frequency for the consideration of torque isolation and a relatively higher vertical natural frequency for the consideration of avoiding shock excitation. This is because the requirements for shock prevention and vibration isolation are conflicting ones. Hence, the selection of natural frequency for a mounting system is only a compromise for the linear elastomeric mounts. Bernard and Starkey (1983) attempted to move the system natural frequency away from an undesired frequency range to reduce the large transferred forces. Swanson *et al*. (1993) showed that the transmitted force could be directly minimized in order to determine a truly optimal design of the mounts. Ashrafiuon (1993) also used these criteria to minimize the dynamic force transmitted from the engine to the body.

The aim of this research is to present analytical as well as finite element model of Budsan truck engine mount system and verify the analytical model to achieve the best stiffness and hystersis damping and reduce the system vibration.

MODELING OF ENGINE MOUNT SYSTEM

For the modeling of engine mount system, the engine is connected to the rigid base structure by rubber mounts and is modeled as a six-DOF rigid body free to translate along and rotate about the three independent Cartesian axes. The center of this coordinate system is located at the center of gravity of the engine and gearbox. The rubber mounts are modeled as springs with the stiffness

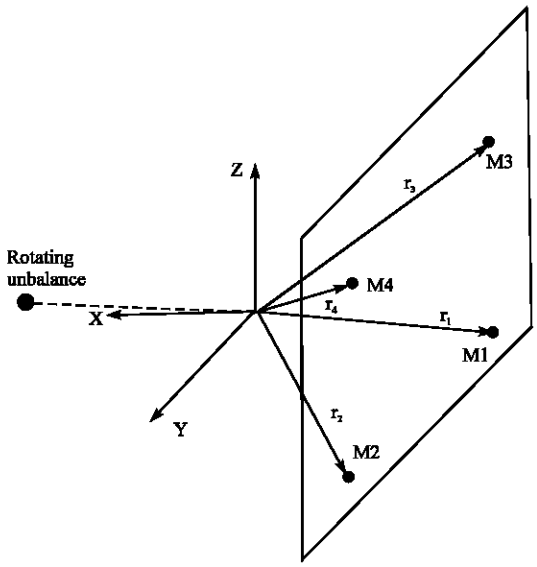

Fig. 2: Configuration of an engine with four mounts

coefficient and a corresponding hystersis damping value in each of three principal directions. Figure 2 shows the configuration of a typical engine-mount system. Using the assumptions above and the Newton's second law, the equation of the motion of system may be written as:

$$M\ddot{U} + C\dot{U} + \bar{K}U = fe^{i\omega t} \quad (1)$$

where, U, $\dot{U}$ and $\ddot{U}$ are the 6×1 displacement, velocity and acceleration vectors, respectively; M is simply the 6×6 engine's rigid mass matrix; $\bar{K}$ is the system's 6×6 complex stiffness matrix; and C is the 6×6 viscous damping matrix which is present only when dampers are also installed between the engine and its base. The right-hand side of Eq. 1 represents a 6×1 vector of harmonic forces and their resulting moments where ω is the forcing frequency. These forces are normally due to the rotating unbalance.

The majority of mounts used in engine mounting applications are a rubber bonded to metal or elastomeric construction. Elastomeric materials behave visco-elastically and for this reason, a complex spring stiffness is used to model the dynamic behavior of the mount; as:

$$\bar{K} = K' + jK'' = K'(1 + i\eta) \quad (2)$$

Where:

K', K'' = Resistive and dissipative spring rates
η = Loss factor

Another interesting characteristic of elastomeric mounts is that they generally possess a higher dynamic

stiffness than static stiffness. To account for this, a dynamic-to-static spring ratio equal to K'/K" is defined. A mount constructed from a purely elastic material will have a loss factor of zero and a dynamic-to static spring ratio of unity.

Based on Eq. 2, the stiffness matrix of an elastic or visco-elastic mounting in its local coordinate system can be written as:

$$\bar{K} = \begin{bmatrix} K'_x + jK''_x & 0 & 0 \\ 0 & K'_y + jK''_y & 0 \\ 0 & 0 & K'_z + jK''_z \end{bmatrix} \quad (3)$$

In this study, in spite of the existence of dampers in the Eq. 1, they don't account for the analytic modeling, because the damping is exerted in complex term of stiffness (Ashrafiuon and Nataraj, 1992). Therefore Eq. 1 can be rewritten as:

$$M\ddot{U} + (K' + iK'')U = fe^{i\omega t} \quad (4)$$

The mass matrix M is shown:

$$M = \begin{bmatrix} m & 0 & 0 & 0 & 0 & 0 \\ 0 & m & 0 & 0 & 0 & 0 \\ 0 & 0 & m & 0 & 0 & 0 \\ 0 & 0 & 0 & I_{xx} & 0 & 0 \\ 0 & 0 & 0 & 0 & I_{yy} & 0 \\ 0 & 0 & 0 & 0 & 0 & I_{zz} \end{bmatrix} \quad (5)$$

Here, m is the mass of engine and gearbox and I_{ii} is tensor elements of inertia.

DYNAMIC ANALYSIS OF ENGINE MOUNT

Vibration is a characteristic of all machinery such as IC engines which have rotating and reciprocating components. It is brought by gas or inertia forces causing stretch in elastic materials, thus energy stored in the elastic deformation- strain energy. The dissipation of this energy and the return to equilibrium is the source of vibration. The way it is stored and/or return to equilibrium is dependent on the characteristics of the engine mount system.

Calculation of the harmonic forces on the cylinder block
Gas pressure forces: The gas pressure forces exerted on the piston area are replaced with one force acting along the cylinder axis and applied to the piston pin axis in order to make the dynamic analysis easier. It is determined for each angle of crank rotation φ. The piston pressure force is:

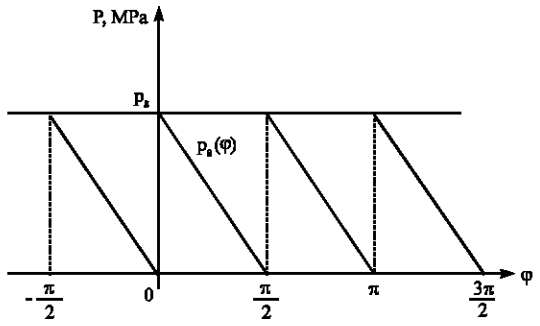

Fig. 3. Combustion pulse in a four-cylinder engine

$$F_g = (p_g - p_o)A_p \quad (6)$$

where, F_g is piston pressure force (MN), A_p is piston area (m^2), p_g and p_o are gas pressure at any moment of time and atmospheric pressure (MPa), respectively (Kolchin and Demidov, 1980).

The gas pressure due to the fuel combustion is in such a way that it is maximized in top dead center of cylinder and decreases by moving the piston downward. In this study, gas pressure curve is assumed to be a saw-tooth. This form can simulate the actual curve of pressure with respect to the crank shaft angle. The combustion pulse in a four-cylinder engine is shown in Fig. 3.

In Fig. 3, the function $p_g(\varphi)$ can be written as:

$$p_g(\varphi) = \frac{2p_g}{\pi}(\frac{\pi}{2} - \varphi) \qquad 0 \le \varphi \le \frac{\pi}{2} \quad (7)$$

where, p_g is the maximum mean effective pressure in the combustion chamber. Because this function is a periodic function with the period of $\frac{\pi}{2}$, it can be represented by expansion of this function by writing its FS as:

$$p_g(\varphi) = \frac{p_g}{2} + \frac{p_g}{\pi}(\sin 4\varphi + \frac{1}{2}\sin 8\varphi + \frac{1}{3}\sin 12\varphi + ...) \quad (8)$$

In a four-cylinder engine the primary forces and moments are balanced whereas the secondary ones are unbalanced. Thus the inertia force for a four-cylinder engine is:

$$P_j = -4m_j R\omega^2 \lambda \cos 2\varphi \quad (9)$$

where, m_j is system of concentrated masses at piston pin (kg), R is crank radius (m), ω is angular velocity (rad sec^{-1}), λ is crank radius to connecting rod length ratio and φ is crank angle. The mass m_j in Eq. 9 is obtained from $m_j = m_p + m_{cp}$, where, m_p is piston mass and

Table 1: Phaser 135-Ti properties of crank mechanism

Parameters	Value (g)	Parameter	Value
Mass of piston	1285.0	Connecting rod length (center by center distance)	219.1 mm
Mass of compress ring No. 1	25.3	Nominal piston cross sectional area	7636 mm^2
Mass of compress ring No. 2	19.7	Radius of crank	63.56 mm
Mass of oil ring	21.3	Maximum of mean effective pressure	1402 MPa
Mass of connecting rod	2090.0		
Mass of piston pin	576.0		
Mass of connecting rod holder	426.0		

$m_{crp} = 0.275\ m_{cr}$ in most existing automobile engines, where, m_{cr} is crankshaft mass.

The total forces acting in a crank mechanism are determined algebraically by adding up the gas pressure forces to the forces of reciprocating masses. According to the properties of crank mechanism of Perkins engine, phaser 135Ti, which is shown in Table 1 (Mireei, 2004) and Eq. 8 and 9, the total force on crank mechanism can be written as:

$$P = P_j+P_g = F_0+F_1\cos\omega_1 t+F_2\sin\omega_2 t+F_3\sin\omega_3 t+ F_4\sin\omega_4 t+... \quad (10)$$

Where:
F_0 = 5352.8 N, $F_1 = -0.1845\ \omega^2$N, F_2 = 3409.4 N, F_3 = 1704.7 N, F_4 = 1136.5 N, $\omega_1 = 2\omega$, $\omega_2 = 4\omega$, $\omega_3 = 8\omega$, $\omega_4 = 12\omega$

Modal analysis of Budsan truck engine mount: Generally, for determination of natural frequencies in the modal analysis, the equation of motion of the system should be solved under homogenous condition, i.e., the solving Eq. 1 with f = 0. To find the natural frequencies of the Budsan track engine mount, first, the mass and stiffness matrices should be determined using Eq. 3 and 5 and then the Eq. 1 must be solved. Table 2 shows the mass and moment of inertia of engine and gearbox for phaser 135Ti engine (Anonymous, 1995).

Using Table 2, mass matrix of equation of motion may be written as:

$$M = \begin{bmatrix} 647 & 0 & 0 & 0 & 0 & 0 \\ 0 & 647 & 0 & 0 & 0 & 0 \\ 0 & 0 & 647 & 0 & 0 & 0 \\ 0 & 0 & 0 & 79.7 & 0 & 0 \\ 0 & 0 & 0 & 0 & 33.02 & 0 \\ 0 & 0 & 0 & 0 & 0 & 86.27 \end{bmatrix} \quad (11)$$

Table 2: Mass and moment of inertia of engine and gearbox for Perkins engine (phaser 135Ti)

Parameters		Values
Mass of engine and gearbox		647 kg
Mass moment of	about x axis	79.7 kg m^2
inertia of engine and gearbox	about y axis	33.02 kg m^2
	about z axis	86.27 kg m^2

Table 3: Static stiffness values in three principal axes

Static stiffness (N m^{-1})	Front engine mount	Rear engine mount
x direction	300.00×10^3	1661.63×10^3
y direction	561.60×10^3	1661.63×10^3
z direction	561.60×10^3	664.65×10^3

To find the stiffness matrix, static stiffness at engine and gearbox loading is determined. Although dynamic to static stiffness ratio may be achieved from manufacturing of engine mounts that is equal to 1.2. Static stiffness values of rear and front engine mounts in three principal axes are shown in Table 3. As mentioned, dissipative or hystersis coefficient of engine mounts must be considered in Eq. 2 to calculate the complex stiffness. This value actually is the difference between loading and unloading curves and is 0.335 for front and 0.242 for rear engine mounts.

Dynamic stiffness of engine mounts in each direction can be determined by multiplying the static stiffness by the dynamic to static stiffness ratio. The total dynamic stiffnesses in three principal directions are:

$$\bar{K}_x = 4707.9\times10^3(1+0.256i) \quad (12)$$

$$\bar{K}_y = 5335.74\times10^3(1+0.266i) \quad (13)$$

$$\bar{K}_z = 2943\times10^3(1+0.285i) \quad (14)$$

Using the directional stiffness, geometric properties of engine and gearbox and moment about each axis, we can write the rotational stiffness about three principal axes. The rotational stiffness about x, y and z axes are:

$$\bar{K}_1 = 268.02\times10^3(1+0.277i) \quad (15)$$

$$\bar{K}_2 = 390.37\times10^3(1+0.296i) \quad (16)$$

$$\bar{K}_3 = 636.48\times10^3(1+0.281i) \quad (17)$$

Therefore $\bar{K}$ is:

$$\bar{K} = 10^3 \times \begin{bmatrix} 4707.9(1+0.256i) & 0 & 0 & 0 & 0 & 0 \\ 0 & 5335.4(1+0.266i) & 0 & 0 & 0 & 0 \\ 0 & 0 & 2943(1+0.285i) & 0 & 0 & 0 \\ 0 & 0 & 0 & 268.0(1+0.277i) & 0 & 0 \\ 0 & 0 & 0 & 0 & 390.4(1+0.296i) & 0 \\ 0 & 0 & 0 & 0 & 0 & 636.5(1+0.281i) \end{bmatrix} \quad (18)$$

Using MATLAB software Ver. 6.5 and writing the mass and stiffness matrices we can get the natural frequencies of the system.

Harmonic analysis of Budsan truck engine mount system: Generally, the displacement of the system can be found by using the mass, damping and stiffness matrices. Hence, for the system with complex stiffness, this displacement can be written by solving the Eq. 4 as:

$$U = \left[K'(1+i\eta) - \omega^2 M\right]^{-1} f \quad (19)$$

where, U is displacement vector, f is disturbance force vector and $\bar{K} = K'(1+i\eta)$ (Eq. 2) is complex stiffness matrix. We use the MATLAB software to determine the system response to the frequency changes from 0 to 200 Hz.

Harmonic analysis of the system using finite element method: In this study, the engine and gearbox is modeled by MPC184 element which is a rigid element in ANSYS software. This element is placed between center of gravity of engine and gearbox and engine mount locations and between engine mounts too. Engine mounts is simulated by Voigt model using spring and damper elements. The spring and damper elements that is used here, is called COMBIN14 element in ANSYS software. The stiffness and damping values are obtained from Budsan engine mount manufacturer. Mass21 element in ANSYS is used to model the mass of the system. Finite element model of Budsan engine mount system is shown in Fig. 4.

Since the total forces on the crank mechanism of engine is a force in y direction, the spring and damper elements are in the y direction. COMBIN14 element is an element with two nodes which define the direction of spring and damper in the model. This element is shown in Fig. 5.

To apply the boundary conditions to the model, the end of spring and damper elements assumed to be fixed (because of rigid chassis assumption) and the connection nodes between spring and damper elements and rigid elements are constrained to the y displacement.

A program is written in ANSYS in such a way that the amplitude of harmonic force is $\tilde{F} = F_0 \sin \omega t$ requested from user and then it is applied to the center of mass (Fig. 6).

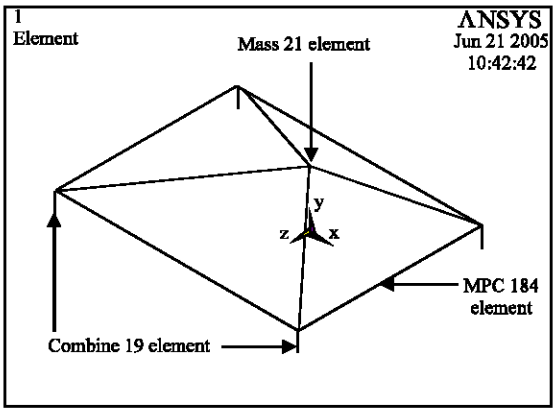

Fig. 4: Finite element model of Budsan engine mount system in ANSYS

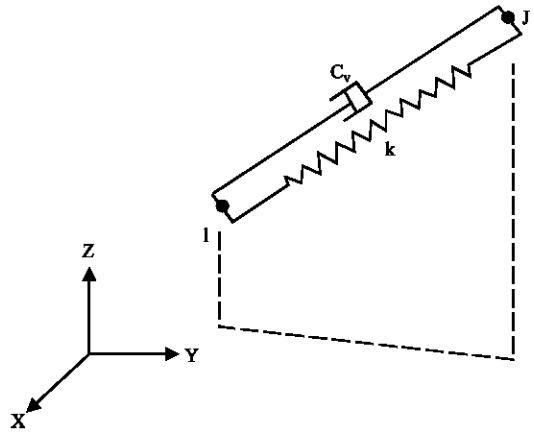

Fig. 5: COMBIN14 element (Anonymous, 2003)

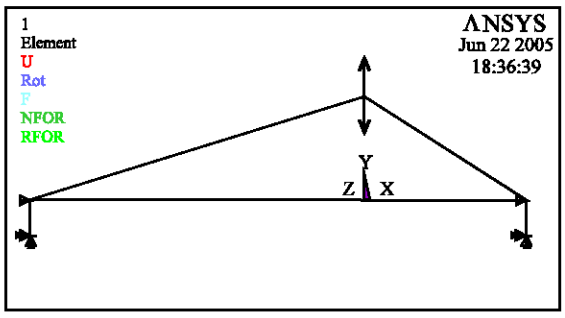

Fig. 6: Applying the boundary conditions and harmonic force

RESULTS AND DISCUSSION

Dynamic forces on a crank mechanism: Since the minimum and maximum of engine speed in this study are 750 and 2600 rpm, respectively, the harmonic frequency range is 12.5 to 43 Hz. Figure 7 shows the harmonic force versus the crank angle at four frequencies 12, 24, 36 and 48 Hz.

As can be seen from Fig. 7, because of increasing the effect of reciprocating part, the harmonic force on cylinder block increases by increasing the engine speed.

Natural frequencies of system: Modal analysis of system was done to determine the natural frequency of the system. Table 4 shows the results obtained for the natural frequency of Budsan truck engine mount system.

Displacement of the system due to the harmonic forces: The harmonic forces were applied to the model to determine the displacement and response of the system. Figure 8 shows the displacement of the system versus the crank angle at four frequencies of 12, 24, 36 and 48 Hz. Figure 9 shows the system response to the frequency.

It is seen from Fig. 8 that the total displacement increases by increasing the frequency (from 12 to 48 Hz). In Fig. 9, at frequency of about 59 Hz, the displacement amplitude increase abruptly. As indicated in Table 4, this frequency is the natural frequency in z direction. The control of displacement in natural frequency is due to the complex term existence in stiffness matrix that expresses the hystersis damping in elastomeric engine mounts (Ashrafiuon and Nataraj, 1992; Ashrafiuon, 1993; Swanson *et al*., 1993).

Harmonic analysis results using FEM: Three terms of harmonic force of Eq. 8 including, $\tilde{F}_2$, $\tilde{F}_3$ and $\tilde{F}_4$ which have sinusoidal waveforms were applied to the finite element model. Figure 10 shows the result of finite element model response to the harmonic force $\tilde{F}_2$.

As can be seen in Fig. 10, natural frequency value in FEM is 58.91 Hz whereas this value in analytical model is

Table 4: Natural frequencies of system (Hz)

Roll	Pitch	Yaw	x	Y	z
ω_1	ω_2	ω_3	ω_4	ω_5	ω_6
111.037	92.378	87.542	86.667	68.774	59.072

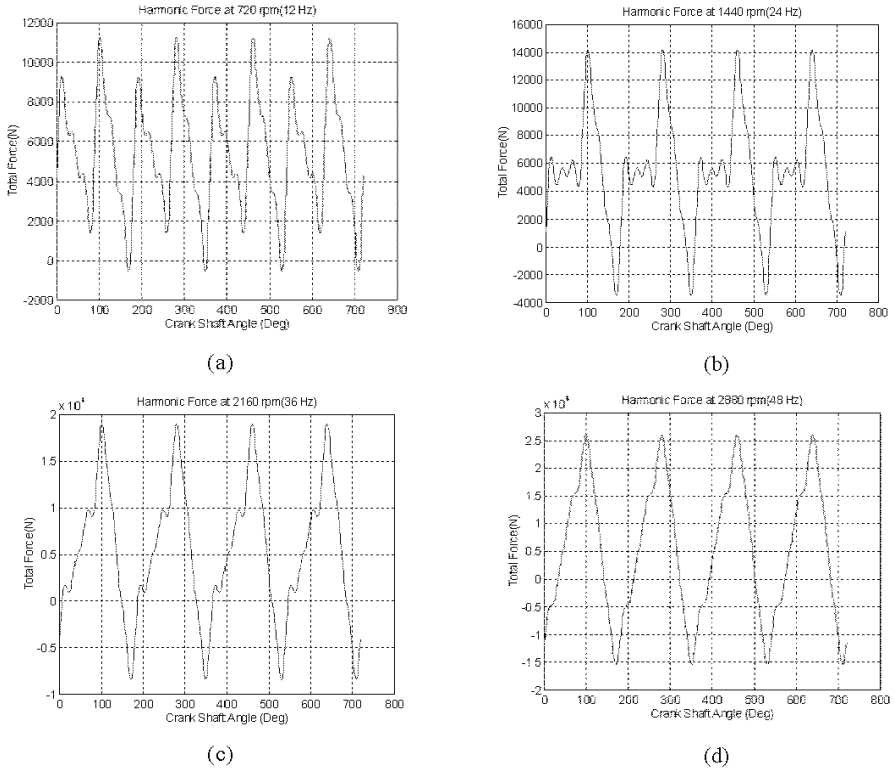

Fig. 7: Total dynamic force in three rotational speed (a) 720, (b) 1440, (c) 2160 and (d) 2880 rpm

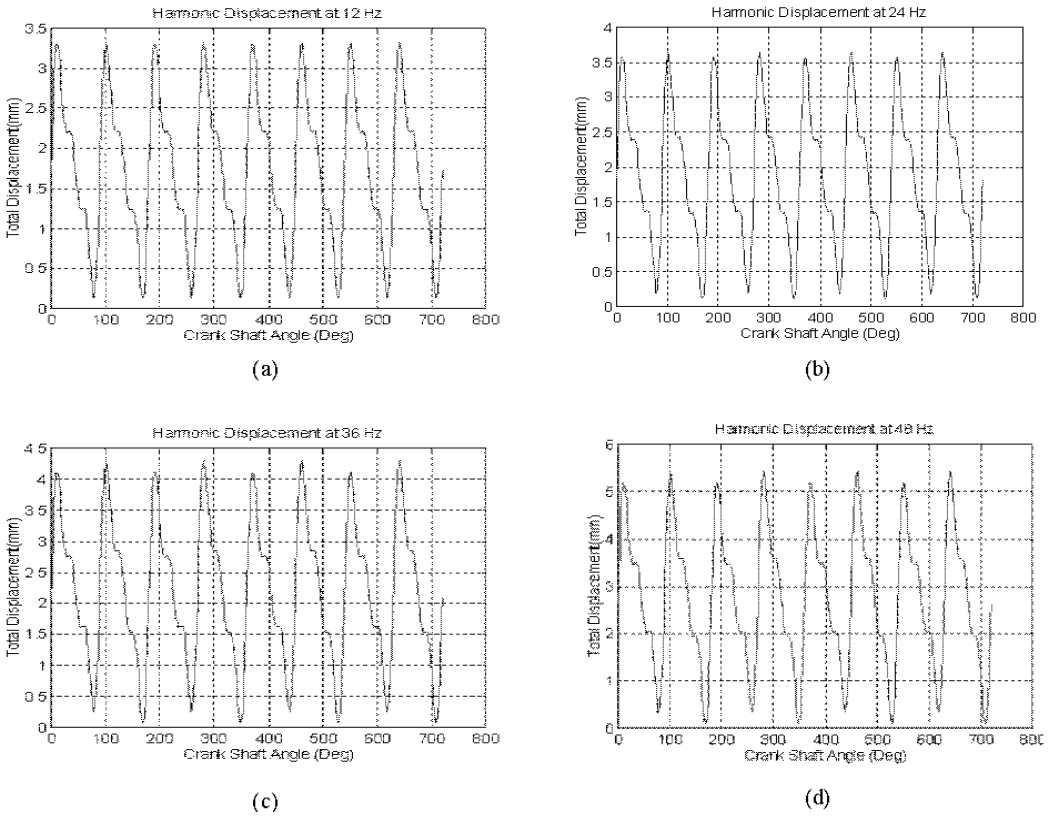

Fig. 8: Displacement of system versus the crank angle in frequencies (a) 12, (b) 24, (c) 36 and (d) 48 Hz

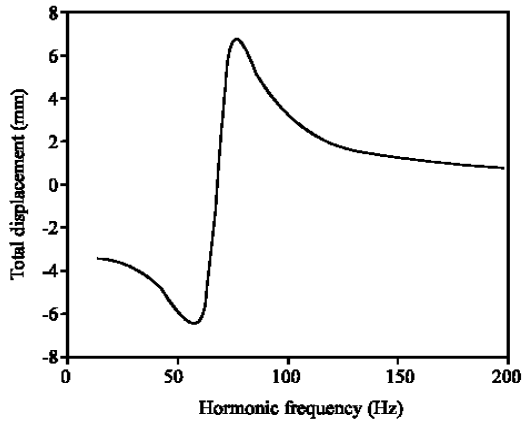

Fig. 9: Displacement versus frequency curve

59.07. Table 5 shows FEM as well as analytic results of system response. The comparison between analytical and numerical solutions shows the fitness of results to state the natural frequency and displacement of system in each analysis and verifies the analytical model. As mentioned, analytical model was based on complex stiffness and zero linear damping whereas the spring and damper model was used in the FEM.

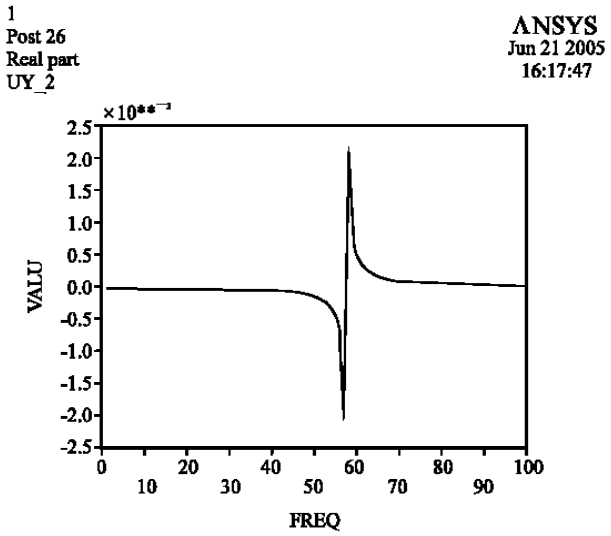

Fig. 10: System response to the harmonic force $\tilde{F}_2$

Optimization: The best stiffness and hystersis coefficients in the z direction should be determined in such a way that the natural frequency of system be far rom the harmonic frequency range (Ashrafiuon, 1993;

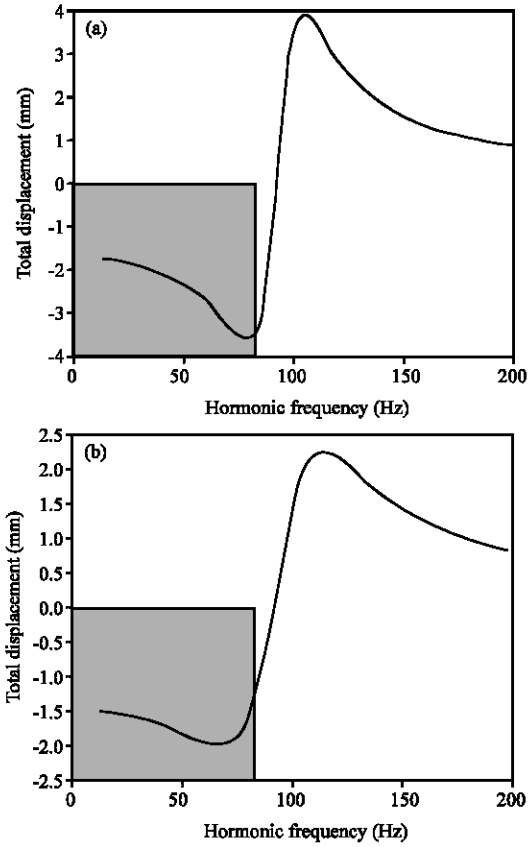

Fig. 11: Optimized engine mount system, a) stiffness 5500 kN and hystersis 0.285 and b) stiffness 5500 kN and hystersis 0.5

Shoureshi *et al*., 1986). Thus to design optimization of a system it is necessary to note: (1) Natural frequency in direction of applied force and (2) Harmonic frequency range. According the modal analysis results, natural frequency of the system in z direction is 59 Hz. Since the engine speed is between 750 to 2600 rpm (12.5 to 43 Hz) and inertia force is $\tilde{F} = F_0 \cos 2\omega t$, thus harmonic frequency range is between 25 to 85 Hz and resonance frequency is:

$$2\omega = \omega_n \Rightarrow \omega = \frac{\omega_n}{2} = \frac{59.07}{2} = 29.54 \text{ Hz} \quad (20)$$

As shown in Fig. 11a, by increasing the stiffness from 2943 to 5500 kN, the natural frequency increases from 59 to 90 Hz and the total displacement reduces from 7 to 3.5 mm. The shaded area indicates the working range of engine. The comparison between Fig. 9 and 11a illustrate that by increasing the stiffness from 2943 to 5500 kN, maximum displacement decreases from 7 to 3.5 mm. However, by increasing the hystersis damping in z direction from 0.285 to 0.5 and stiffness to 5500 kN, the total displacement could be reduced from 3.5 to 2 mm as shown in Fig. 11b. Thus, despite of limitations and trial and error method we can conclude that the optimized stiffness and hystersis damping for the Budsan engine mount system are 5500 and 0.5 kN, respectively. With these values, the total displacement could be reduced from 7 to 2 mm.

Table 5: Comparison between analytical and numerical results

	System response to $\tilde{F}_2$		System response to $\tilde{F}_3$		System response to $\tilde{F}_4$	
	Analytic	Numeric	Analytic	Numeric	Analytic	Numeric
Displacement (mm)	2	2.1	0.98	1.1	0.66	0.7

CONCLUSION

It is concluded that analytical engine mount model based on complex stiffness and zero linear damping has a good fitness in results by finite element model based on spring and damper model. After verification of analytical model by finite element model we applied it to optimize the Budsan truck engine mount system. In this way, by increasing the stiffness from 2943 to 5500 kN and hystersis damping in z direction from 0.285 to 0.5, it is possible to reduce the total displacement from 7 to 2 mm.

ACKNOWLEDGMENT

The authors would like to thank Research Deputy of University of Tehran for its financial support.

REFERENCES

Anonymous, 1995. Hand Book of Perkins Engines. Perkins Group Limited.

Anonymous, 2003. ANSYS User Guide. ANSYS Group, Ver. 8.

Arai, T., T. Kubozuka and S.D. Gray, 1993. Development of an engine mounts optimization method using modal parameters. SAE Paper: 932898.

Ashrafiuon, H. and C. Nataraj, 1992. Dynamic analysis of engine-mount systems. J. Vibration Acoust., 114 (1): 79-83.

Ashrafiuon, H., 1993. Design optimization of aircraft engine-mount. J. Vibration Acoust., 115 (4): 463-467.

Bernard, J.E. and J. Starkey, 1983. Engine Mount Optimization. SAE Paper: 830257.

Browne, K.A. and E.A. Taylor, 1939. Engine Mount. US Patent: 2175285.

Bucksbee, J.H., 1987. The Use of bonded elastomers for energy and motion control in construction. J. Rubber World, 196 (1): 38-45.

Geck, P.E. and R.D. Patton, 1984. Front wheel drive engine mount optimization. SAE Paper: 840736.

Johnson, S.R. and J.W. Subhedar, 1979. Computer optimization of engine mounting systems. SAE Paper 790974.

Kolchin, A. and V. Demidov, 1980. Design of Automotive Engines. MIR Publisher, Moscow.

Mireei, S.A., 2004. Dynamic and vibration analysis of Budsan truck engine mount and design a vibration reduction system. M.Sc. Thesis, University of Tehran, Iran.

Shoureshi, R., P.L. Graf and T.L. Houston, 1986. Adaptive engine mounts. SAE Paper: 860549.

Swanson, D.A., 1992. Active engine mounts for vehicles. SAE Paper: 932432.

Swanson, D.A., H.T. Wu and H. Ashrafiuon, 1993. Optimization of aircraft engine suspension system. J. Aircraft, 30 (6): 979-984.

Yu, Y., N.G. Naganathan and R.V. Dukkipati, 2000. A literature review of automotive engine mounting systems. J. Vehicle Design, 24 (4): 32-57.